Journal of Molecular Graphics and Modelling 27 (2008) 452–458

Contents lists available at ScienceDirect

Journal of Molecular Graphics and Modelling

journal homepage: www.elsevier.com/locate/JMGM

Molecular basis of agonicity and antagonicity in the androgen receptor studied by molecular dynamics simulations

William H. Bisson [a,1], Ruben Abagyan [a], Claudio N. Cavasotto [b,*]

[a] The Scripps Research Institute, 10550 North Torrey Pines Road, La Jolla, CA 92037, United States
[b] School of Health Information Sciences, University of Texas Health Science Center at Houston, 7000 Fannin #860B, Houston, TX 77030-5400, United States

ARTICLE INFO

Article history:
Received 30 June 2008
Received in revised form 30 July 2008
Accepted 2 August 2008
Available online 9 August 2008

Keywords:
Nuclear receptor
Androgen receptor
Molecular dynamics
Passive antagonism
Prostate cancer
Flutamide
Bicalutamide

ABSTRACT

Treatment of prostate cancer patients with antiandrogens is initially successful, though the therapy often becomes refractory over the time. This mechanism is not fully understood, but the presence of androgen receptor (AR) mutant forms which are activated by antiandrogens and other endogenous ligands, and overexpression of the receptor have been suggested. In an attempt to explain the molecular basis for agonicity and antagonicity in the androgen receptor, and the changes on biological activity of subtle modifications at the ligand and receptor (mutations) level, molecular dynamics simulations were performed on the androgen receptor wild type (WT), and T877A and W741 mutant forms, complexed with several non-steroidal androgens. The stabilizing role of residues from helices 3, 5, 11 and 12 was observed in non-steroidal androgens *R*-3, *S*-1, and *R*-bicalutamide and hydroxyflutamide in resistant mutations. In the AR WT antiandrogen *R*-bicalutamide complex, destabilization of M895 by both W741 and the sulfonyl linkage of the ligand may be responsible for reported antagonism. Changes in the ligand or mutations alleviating this effect were observed to stabilize the receptor in the active conformation, thus developing resistance to *R*-bicalutamide. The results presented provide a plausible explanation for the molecular basis of agonicity and antagonicity in the androgen receptor, and complement previous studies using static crystal structures, incorporating for the first time protein dynamics into the analysis. Thus, our results provide a valuable framework for the structure-based design of improved antiandrogens.

© 2008 Elsevier Inc. All rights reserved.

1. Introduction

The androgen receptor (AR) regulates the proliferation of prostate tumor cells and is a well-established target for the treatment of human prostate cancer (PCa) [1]. Treatment of PCa includes surgical androgen ablation followed by blocking the remaining levels of AR activity with steroidal antagonists such as chlormadinone acetate and megestrol acetate, or with non-steroidal antagonists as hydroxyflutamide (HF) and *R*-bicalutamide [2]. Though treatment is initially successful, prostate cancer becomes later on often refractory to antiandrogens. This mechanism is not yet fully understood, but altered specificity of mutated forms of AR -towards which antiandrogens exhibit androgenic activity, and overexpression of AR have been suggested [2].

The AR is a member of the nuclear receptor (NR) superfamily, and is characterized by three major domains: the N-terminal (which contains the ligand-independent activation function-1 domain), the DNA binding domain, and a C-terminal ligand binding domain (LBD) [3], which controls transcription in a ligand-dependent manner.

A number of mutations have been reported for the AR in prostate cancer tumor cells [http://www.mcgill.ca/androgendb/] and their location and function may help us to understand how androgen-independent PCa occurs and should be treated. The majority of the mutations are confined to the LBD. In particular, mutations T877A and W741L/C were identified in patients after the initial treatment with the clinical antiandrogens flutamide and *R*-bicalutamide, respectively. Recently, Hara et al. [4] demonstrated that after weeks of bicalutamide treatment, LNCaP cells reveal novel additional point mutation at codon 741 (Trp to Cys or Leu), which makes bicalutamide act as an agonist towards AR. Mutation T877A, predominantly found in metastatic tumors [5], makes the AR more promiscuous and allows it to be activated by other endogenous ligands such as progesterones and estrogens [5],

* Corresponding author. Tel.: +1 713 500 3934; fax: +1 713 500 3929.
E-mail address: Claudio.N.Cavasotto@uth.tmc.edu (C.N. Cavasotto).
[1] Current address: 1007 Agriculture and Life Sciences Building, Oregon State University, Corvallis, OR 97331, United States.

1093-3263/$ – see front matter © 2008 Elsevier Inc. All rights reserved.
doi:10.1016/j.jmgm.2008.08.001

and even by AR wild type (WT) antiandrogens like hydroxyflutamide (HF) and others [6]. Residues T877 and W741 are located in the receptor's binding site, and could therefore be important for ligand specificity [7]. A double mutant AR, T877A/L701H has been shown to be activated also by glucocorticoids [8].

Structural data from nuclear receptors [9] revealed that upon agonist binding, helix 12 (H12) adopts a position favorable to co-activator binding, what is believed to trigger co-factor recruitment, macromolecular assembly, and initiate transcription. Many of the NR antagonists have bulky moieties which precludes H12 to adopt the proper position for co-activator recruitment, thus silencing transcription. This mechanism of action is called active antagonism [10]. However, some antagonists that lack the bulky substituent such as THC (*R*,*R* 5,11-*cis*-diethyl-5,6,11,12-tetrahydrochrysene-2,8-diol) for the estrogen receptor β (ERβ) [10], and progesterone for the mineralcorticoid receptor (MR) [11] most likely exert their effect in a more subtle way. This mechanism of action was first called passive antagonism by Shiau et al. [10], who from the solved THC/ERβ crystal structure, pointed out that THC antagonizes ERβ by stabilizing a non-productive receptor conformation, and not by directly precluding H12 to adopt the agonist bound pose.

The subtle effect of mutations in ligand agonicity/antagonicity, and passive antagonism cannot be rationalized as a simple on/off switch mechanism, and it is thus clear that in some cases, activation/inhibition of NRs could be a much more complex process, whereby the presence of mutations and passive antagonists may shift the equilibrium towards more active or inactive conformations of the receptor, where the concentration of co-activators and co-repressors may play an important role (cf. the excellent review of Nagy and Schwabe [12]). Computational tools have been used in the past to explore ligand:receptor dynamics at an atomic level. Carlsson et al. analyzed through molecular dynamics (MD) why the GR V571M mutant is more sensitive to aldosterone than the GR WT [13]. The simulations showed that the V571M mutation induces re-arrangement in the AF-2 region of the GR, thus making the receptor-co-activator interaction energetically more favorable. Burton and co-workers showed through comparing the MD simulations of three different GR systems, unbound, bound to agonist dexamethasone, and to passive antiglucorticoid 21-hydroxy-6,19-epoxyprogesterone, that the latter exerts its antagonicity by inducing fluctuations in the H1–H3 loop, thus affecting the ability of the receptor to homodimerize, a necessary step to initiate transcription [14]. Other studies include the influence of the binding site structure in ERα dynamics [15], ER selectivity [16], and the determination of the influence of ligand binding on the dynamics of the liver receptor homologue 1 [17].

Recently, Bell, Dalton and co-workers published several crystal structures of the AR WT and mutant forms complexed with non-steroidal ligands, thus providing for the first time clues about agonist/antagonist modulation in AR and its most common mutations [18–20].

The present work approaches the same problematic but incorporating protein dynamics into the picture, exploiting the potentiality of MD simulations in a fully solvated environment. Our goal is to investigate the molecular basis of agonicity and antagonicity in the AR, and the impact on the biological activity of subtle changes in the ligand and/or the receptor (mutations). The ligands investigated were the natural agonist dehydrotestosterone (DHT), the non-steroidal HF and *R*-bicalutamide, and two of their derivatives treated by Bell, Dalton and co-workers in their work [19], *R*-3 and *S*-1 (Scheme 1). The dynamics of the ligand:AR complexes in the WT, and T877A and W741L mutant forms were investigated by 2.15 ns MD.

The results obtained offer, for the first time incorporating protein dynamics, a plausible explanation for the molecular mechanism of action of non-steroidal androgens and antiandro-

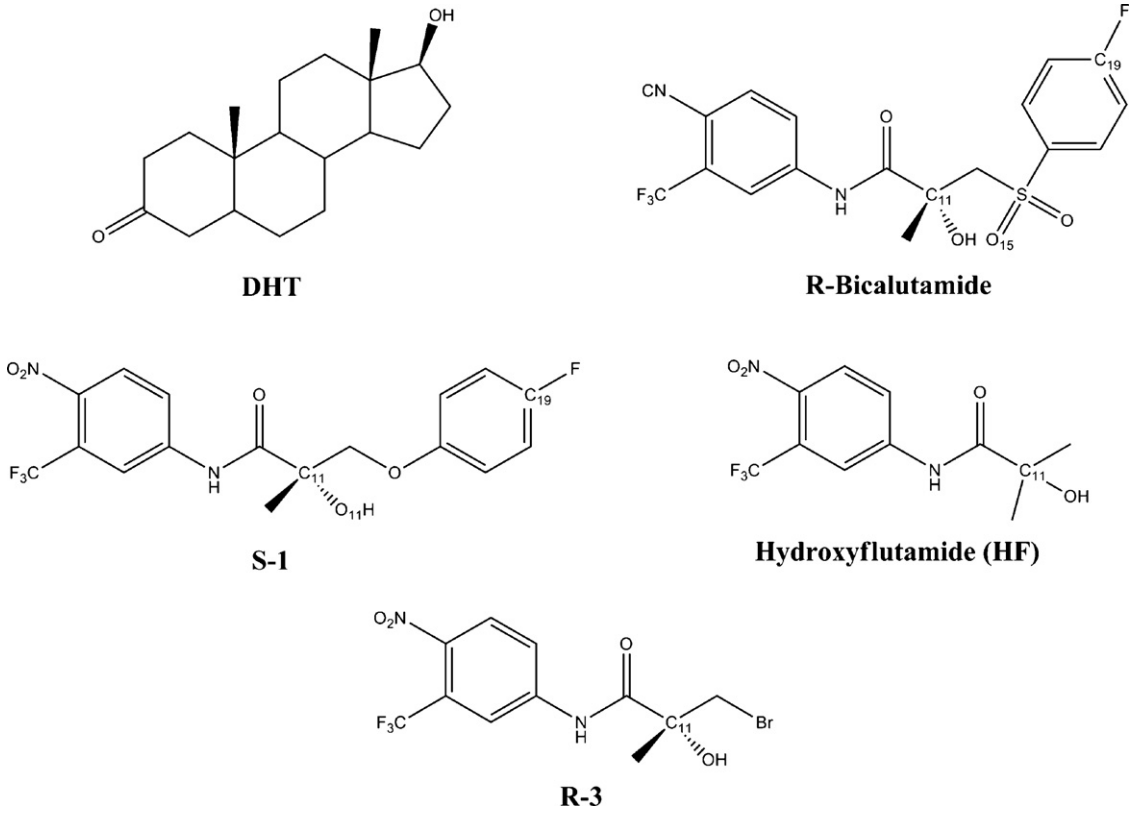

Scheme 1. Chemical structures of dehydrotestosterone (DHT), *R*-bicalutamide, hydroxyflutamide (HF), and HF derivatives *R*-3 and *S*-1.

gens in the AR WT and mutant forms. This would provide a valuable framework for structure-based design of ligands which antagonize both the AR and selected mutants.

2. Methodology

2.1. Preparation of the ligand:AR complexes

The 3D coordinates of ligand: AR complexes were taken from crystal structures PDB IDs: 1Z95 (*R*-bicalutamide/W741L), 2AX9 (*R*-3/WT), 2AX6 (HF/T877A), 2AXA (*S*-1/WT), 2AX8 (*S*-1/W741L), 1I37 (DHT/WT). The structures of DHT, bicalutamide, HF, *R*-3 and *S*-1 are shown in Scheme 1. The complexes between *R*-bicalutamide and HF with AR WT were prepared using flexible-ligand:flexible-receptor-docking from the 1I37 structure, as already reported [21] (see Refs. [22–24] for description of the methodology).

2.2. Molecular dynamics simulations

The preparation of files of DHT, bicalutamide, hydroxyflutamide, *R*-3 and *S*-1 were performed using the program ANTECHAMBER and LEAP. All models were immersed in a box of water molecules and Cl^- counterions were added to the solvent bulk of the protein/water complexes to maintain neutrality of the system using program AMBER8 [25]. Periodic boundary conditions were applied. The Amber force field all atom parameters (parm94) was used. The minimization protocol consisted in 1000 cycles of steepest descent followed by conjugate gradient method until the root-mean square deviation (RMSD) of the Cartesian elements of the gradient reached a value smaller than 0.15 Å.

The dynamic protocol consisted in three steps MD1, MD2 and MD3. The initial temperature for MD1, MD2 and MD3 was set respectively at 0, 150, 300 K. During all dynamic steps the reference temperature at which the system had to be kept was 300 K according to Berendsen's coupling algorithms [26]. The time step for all three dynamic procedures was 0.002 picosec (ps). For minimization and MD, the primary cutoff distance for non-bonded interaction was set at 9 Å. Regarding the MD protocol used, the first (MD1) aimed the equilibration of water molecules and ions of the water boxed and charge neutralized model. An initial velocity was given to the system and then trajectories were allowed to evolve in time according to Newtonian laws keeping the model protein fixed. The number of dynamics steps was 7500 corresponding to 15 ps. Then, 15 ps of constant volume dynamic (MD2) was performed on the all system to adjust density to a value of 1. In the third step a 500 ps constant pressure dynamic (MD3) at 1 atm was applied without any constraint to finally assess conformational stability.

The AMBER package has been successfully used to study ligand:protein interaction in different systems like TIBO derivatives binding to HIV-1 RT [27] and HIV protease drug resistance [28], and also in ligand:NR interaction, such as xenoestrogens binding to the ER [29], passive antagonism in GR [14], and the effect of AR mutations in androgen insensitivity syndrome [30], among others.

3. Results and discussion

In order to investigate the molecular basis of agonicity/antagonicity activity of non-steroidal ligands in AR WT, and mutations T877A and W741L, we performed MD simulations on several models in the presence of explicit solvent molecules. The following models were studied (see Table 1): AR WT complexed with non-steroidal agonists *R*-3 (model **1**), *S*-1 (model **2**), AR WT steroid agonist DHT (model **4**), AR WT antagonists *R*-bicalutamide (model **5**) and HF (model **7**); the AR W741L mutant form complexed with agonists *S*-1 (model **3**) and *R*-bicalutamide (model **6**); the AR T877A mutant with agonist HF (model **8**). Since no crystal structure of the AR in the antagonist bound conformation is available, agonist-bound structures are used as initial structures in models **5** and **7**, analyzing in this study the structural and dynamical effects of antagonists bound to them. A similar approach has been taken for the analysis of passive antagonism in GR [14]. A computational study on AR has been already reported [31]; however, the models were built from the human progesterone receptor (PR) due to the lack of AR structural information at that time, and with a shorter simulation time (300 ps compared to 2.15 ns in this study).

Table 1
The eight human AR ligand binding domain complexes analyzed through molecular dynamics

Model no.	AR mutant form	Ligand
1	WT	*R*-3
2	WT	*S*-1
3	W741L	*S*-1
4	WT	DHT
5	WT	*R*-Bicalutamide
6	W741L	*R*-Bicalutamide
7	WT	Hydroxyflutamide
8	T877A	Hydroxyflutamide

The RMSD as a function of time of all models shows that a plateau, representing stable conformation over time, was reached after circa 1 ns MD (see Supplemental Information). The low RMSD of around 1.75 Å and structural comparison along the simulation time indicates that the starting X-ray structure represents a stable conformation, and the MD protocol is suited to assess the stability of the models.

3.1. Molecular basis for the AR WT agonicity of non-steroidal R-3, a derivative from antagonist HF

The HF derivative *R*-3 (see Scheme 1), an agonist towards the AR WT, differs from its parent structure by the substitution of a methyl group with a bulkier methylbromine group which gives origin to a stereochemical center (*R* is the active enantiomer). MD of the *R*-3/AR WT complex (model **1**) showed that the hydroxyl group of *R*-3 established a stable hydrogen bond interaction with the carbonyl oxygen of the side chain of N705 (located in H3) throughout the simulation, as found with HF and *R*-bicalutamide in the T877A and W741L mutant, respectively (see below). Compared to its position when bound to steroidal ligands [32], the side chain of T877 (in H11) is flipped 180° towards L873, and did not interact with the ligand throughout the simulation, although *R*-3 and T877 exhibit stable van der Waals contacts. This confirms the common tendency of non-steroidal ligands to avoid hydrogen bond with this residue upon binding to the AR-LBD [19].

The bromine atom of *R*-3 is surrounded by and in contact with the side chains of W741 and M742, which form a stable bulky shell around it with poor mobility of the H5 surrounding the binding pocket (see Supplemental Information). It was also observed that the side chain of M895 (located in H12) is partially in contact with the Br atom, but assuming a more dynamic conformation (see Fig. 1 and Supplemental Information). This is in agreement with the higher B-factor reported for the side chain of M895 in the *R*-3/AR WT crystal structure [19]. As a consequence, the replacement of M895 and W741 should have an effect in the stability of *R*-3 in the agonist conformation as it really happens experimentally with the W741L and M895T AR mutations [19]. Moreover, the difference in the degree of interaction between *R*-3–W741 and *R*-3–M895

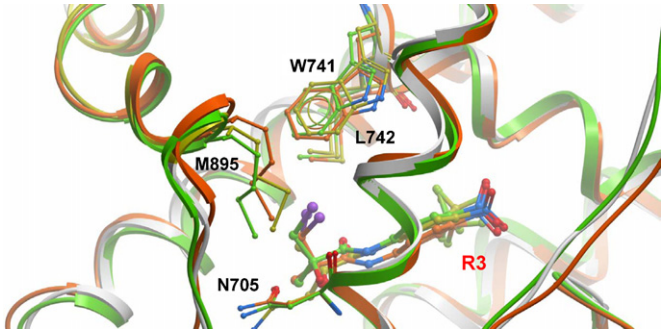

Fig. 1. Snapshots taken from model **1** (*R*-3/AR WT) at 1.6, 1.8 and 2.0 ns. *R*-3 carbon atoms, residues and ribbons are colored yellow (1.6 ns), green (1.8 ns) and orange (2.0 ns). Oxygen atoms are displayed in red, nitrogens in blue.

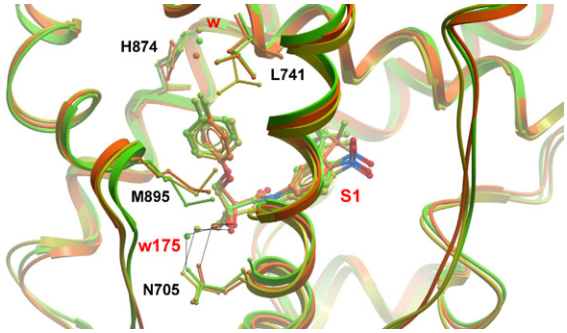

Fig. 2. Snapshots taken from model **3** (*S*-1/AR W741L) at 1.6, 1.8 and 2.0 ns. *S*-1 carbon atoms, water molecules, residues and ribbons are colored yellow (1.6 ns), green (1.8 ns) and orange (2.0 ns). Oxygen atoms are displayed in red, nitrogens in blue. The hydrogen bonds are displayed as black dashed lines.

correlates with the degree of transcriptional activation loss reported in W741L and M895T, respectively [19]. Mutation T877A is likely to have no effect in the cage surrounding the Br atom in *R*-3, and the probable presence of a water molecule bridging the ketone oxygen in *R*-3 with the backbone oxygen of L873, analogue to the one found in AR T877A complexed with HF (PDB ID: 2AX6) and *S*-1 (PDB ID: 2AX7), may account for the increased agonist activity of *R*-3 in the AR T877A mutant.

3.2. Study of the interactions between AR WT and W741L with non-steroidal agonist S-1, an analog to AR WT antagonist R-bicalutamide

The *R*-bicalutamide derivative *S*-1 is an agonist towards both the AR WT and AR W741L mutant form. To understand the mechanism of action of *S*-1 and its sustained activity in AR mutations, we performed MD simulations of *S*-1 complexed in both receptors (models **2** and **3**, respectively).

In the WT the hydrogen bond of the hydroxyl group of *S*-1 with the carbonyl oxygen of the side chain of N705 remained stable during the entire simulation time. As in model **1**, no hydrogen bond was detected between the ligand and T877 in both the WT and W741L mutation, though van der Waals contacts were present. Like the other cases, the stability of the hydrogen bond network around the NO_2 (involving R752 and several water molecules) was confirmed in both models (**2** and **3**). In model **2**, and from the analysis of the ligand: receptor contacts of *S*-1 chiral carbon (C_{11}) and the B-ring (C_{19}), we observed that residues W741, M742, H874, I899 make a stable shell around the B-ring portion of *S*-1 (see Supplemental Information), thus helping in stabilizing the ligand in the complex, as it has been already hypothesized [19]. In addition, π–π stacking (W741/*S*-1) may add stability to the system. The B-ring shows a stable conformation similar to that of *R*-bicalutamide in the AR W741L mutation, and in agreement with crystal structures [18,19] (PDB ID: 2AXA and 1Z95). Residue M895 packs closely against *S*-1, being stable during the simulation, and in agreement with the low B-factor reported in the crystal structure (PDB ID: 2AXA). Loss of contact with the ligand upon the M895T substitution may thus explain the reduce agonist activity of *S*-1 observed in this mutation [19].

In the W741L mutant (model **3**), however, the side chain of M895 is more mobile (see Supplemental Information), in agreement with the higher B-factor reported for this crystal structure (PDB ID: 2AX8). It moves towards L741 and opens space for a water molecule (w175), which becomes the center of a hydrogen bond network, involving the side chain of N705 and the hydroxyl group of *S*-1 (see Fig. 2). The incorporation of w175 replaces the loss of interaction between M895 and *S*-1. It is observed, however, a slightly decreased interaction between the B-ring of *S*-1 and L741, when compared to W741 (cf. Supplemental Information). Water molecule w175 is neither present in the *S*-1/WT complex due to the close contact between *S*-1 and M895, nor in the *R*-bicalutamide/AR W741L complex, because of the presence of the bulkier sulfonyl group. The increased agonist activity of *S*-1 towards the T877A mutation [19] could be rationalized in an analogous way as with *R*-3, by means of the water bridging the ligand and L873, located in H11.

It is interesting to note that contrary to what has been hypothesized [19], no internal hydrogen bond is observed between the amide hydrogen and the ether linkage in *S*-1 in models **2** and **3**, as the O···H distances are on average 2.6–2.8 Å (Fig. 3).

Thus, in both models **2** and **3**, it is observed that the ligand establishes key contacts with residues in H3, H5, H11 and H12, what provides stability to the system.

3.3. Comparison of DHT and non-steroidal agonists binding to AR

During 2.15 ns MD, AR WT complexed with DHT (model **4**) showed conformational stability, establishing hydrogen bonds with the side chain of N705, T877 and R752, and confirming the hydrogen bond network already reported [31,32].

The role of the stabilizing hydrogen bond between the ligand and the side chain of N705 in the non-steroidal agonists *R*-3 and *S*-1 has been described above (models **1** and **2**). We observed that after 515 ps MD the hydroxyl group of *R*-3 and *S*-1 points towards the carbonyl oxygen of N705 and the hydrogen bond established remains stable for the entire simulation time of 2.15 ns. However, in those models, there is no hydrogen bond interaction with T877. This states a clear difference between steroidal and non-steroidal agonist in the interaction with the side chain of T877, which is absent in the second case, as already observed [19].

3.4. Analysis of the antagonist-to-agonist switch of R-bicalutamide upon the AR W741L mutation

R-Bicalutamide is an antagonist towards the AR WT, but an agonist towards the W741L mutant form. To better understand the molecular basis for this change, MD simulations were performed on AR WT (model **5**) and AR W741L (model **6**) complexed with *R*-bicalutamide.

In model **6**, the hydroxyl group of *R*-bicalutamide establishes a hydrogen bond with the carbonyl oxygen of the side chain of N705 (H3). The stability of the hydrogen bond network around R752 and the cyano group in *R*-bicalutamide is confirmed by MD. No hydrogen bond was observed in AR W741L between *R*-bicalutamide and Q711 throughout the simulation, in agreement with what has been already proposed [18]. Unlike DHT, but similar to

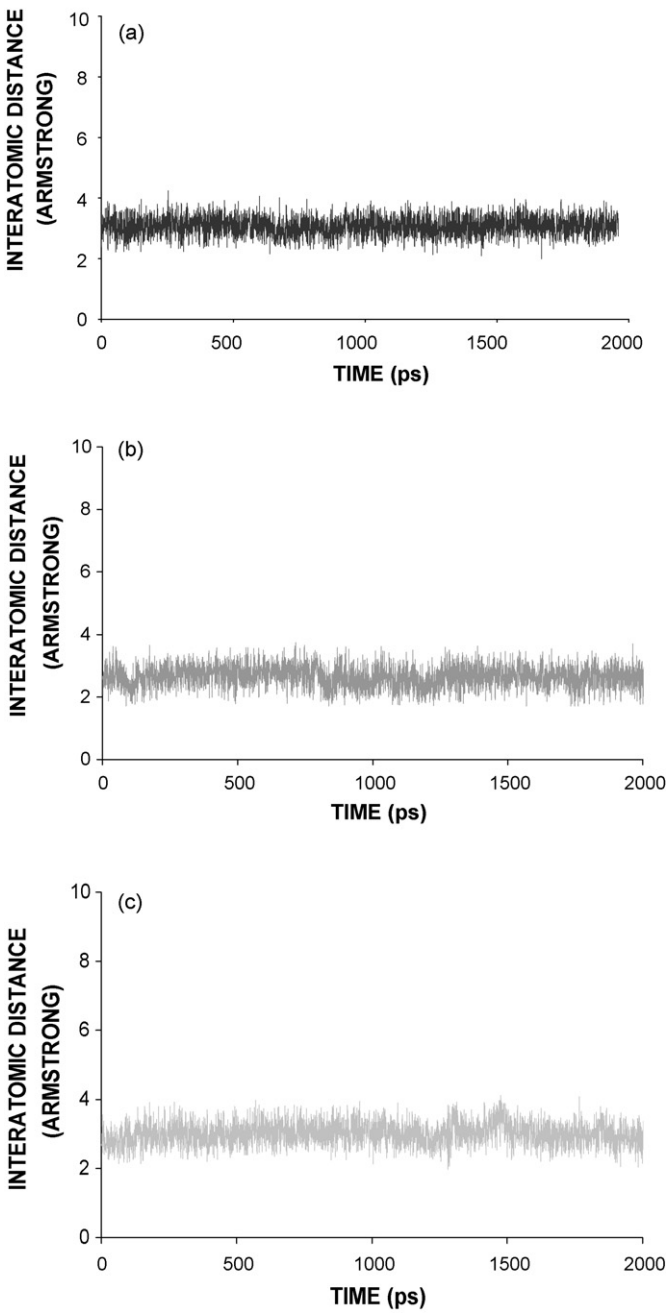

Fig. 3. Evolution of the intramolecular hydrogen bond distances during 2.15 ns of MD in the complex between *R*-bicalutamide and AR W741L (model **6**), and *S*-1 with WT and AR W741L (models **2** and **3**, respectively). Initial time (t = 0 ps) is measured after minimization stage (see Section 2). Color code: Black, NH···O=S (*R*-bicalutamide, model **6**); dark grey (model **2**) and light grey (model **3**) NH···C–O–Ar (*S*-1).

models **1**–**3**, no hydrogen bonding between the ligand and T877 (H11) is observed, but stable van der Waals contacts. In the WT (model **5**), the contacts between the cyano group and neighbouring residues (R752, N705) are highly similar to those of W741L, exhibiting the same pattern throughout the simulation.

We noticed that M895 is more mobile in the *R*-bicalutamide complex with WT than in the W741 mutant form, adding a destabilizing factor to H12. In the complex with the W741L mutant, however, M895 is able to pack towards *R*-bicalutamide. The evolution of key interaction distances between the ligand and

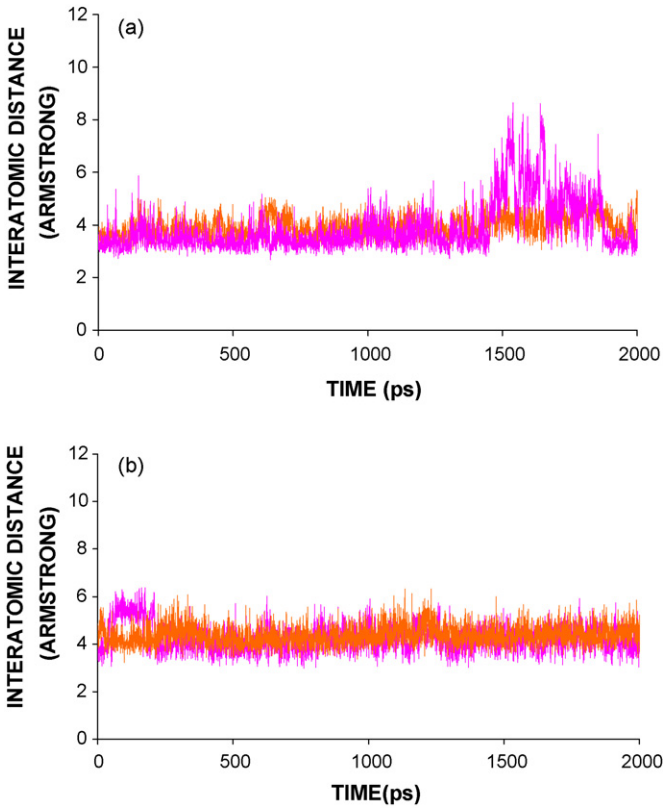

Fig. 4. Evolution of interatomic distance during 2.15 ns of MD in the complex *R*-bicalutamide (Bic) and (a) WT and (b) W741L AR-LBD. Initial time (t = 0 ps) is measured after minimization stage (see Section 2). Color code: (a and b) Purple, O_{15} Bic—C_{ε} M895; orange, C_{19} Bic—CH_{ind} W741 (WT) and $C_{\delta 1}$ L741 (W741L).

the receptor are depicted in Fig. 4 and Supplemental Information. Clearly, the interaction between the ligand and the residue at position 741 (W or L) is stable in both cases, as it can be seen from the evolution of the interaction between the B-ring (C_{19}) and C_{11} with the side chain of W/L741. As it has been already suggested [19], we confirm that the equilibrium towards the agonist conformation in the mutant form could be also helped by the presence of the water molecule closed to H874 which provides a stable environment around the sulfonyl-linked phenyl B-ring of *R*-bicalutamide which as a consequence remains stable and in contact with L741 (see Fig. 5). No internal hydrogen bond is observed in the *R*-bicalutamide/AR W741L complex between the amide hydrogen and the sulfonyl oxygen (Fig. 3), consistent with what it was seen in models **2** and **3**.

In the AR WT, thus, M895 is pushed away both by W741 and the sulfonyl linkage, loosing packing onto *R*-bicalutamide and most likely unstabilizing H12. This could make receptor:co-activator interaction energetically unfavorable, in a similar way as shown upon the V571M mutation in GR [13]. Thus the steric preclusion of M895 by the sulfonyl group and by W741 could explain *R*-bicalutamide antagonism in the WT, and not the clash of *R*-bicalutamide with W741. That instability could be alleviated in different ways, thereby resulting in AR activation: (i) with a less bulkier linker, like in AR WT agonist *S*-1, thus allowing the side chain of M895 to pack closely to the ligand (as we observed in model **2**); (ii) by a substitution with a smaller residue, like the *R*-bicalutamide resistant mutation M895T [19]; (iii) in an indirect way, like the AR W741L mutation, towards which *R*-bicalutamide acts as an agonist, and where M895 gets its stability by packing towards L741 (cf. model **5**).

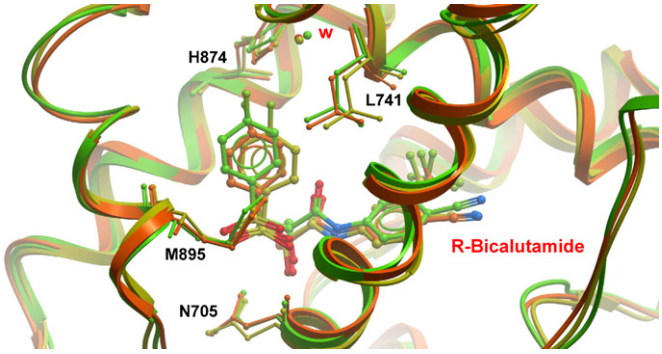

Fig. 5. Snapshots taken from model **6** (*R*-bicalutamide/AR W741L) at 1.6, 1.8 and 2.0 ns. *R*-Bicalutamide carbon atoms, water molecules, residues and ribbons are colored yellow (1.6 ns), green (1.8 ns) and orange (2.0 ns). Oxygen atoms are displayed in red, nitrogens in blue.

3.5. Analysis of the antagonist-to-agonist switch of HF upon the AR T877A mutation

To analyze why HF switches its activity from antagonist to agonist upon the T877A mutation, we performed 2.15 ns of MD simulations of the WT and T877A mutant form bound to HF (models **7** and **8**, respectively).

In both WT and mutant T877A the hydrogen bonding between the hydroxyl group of HF and the carbonyl oxygen of the side chain of N705 (H3) remained stable during the entire period of 2.15 ns. The hydrogen bond network involving R752 and the nitro group of HF also displayed stability throughout the simulation.

Analysis of the interaction distances throughout the simulation showed a weaker interaction between the ligand and M895 (H12) in the WT compared to the T877A AR mutant, and a slightly better stability of the mutant form in terms of mobility of the H12 with respect to the ligand (cf. Supplemental Information). This has to be compared to the complex between AR WT and *R*-3 (model **1**), where the Br atom in the latter helps stabilize the contact between the ligand and M895, which may be critical for the stability of the complex. The water molecule present in the T877A mutant bridging L873 and HF adds stability to the complex linking the ligand with H11. Model **8** also displays a stronger interaction between HF and M895 (H12) (cf. Supplemental Information). Remarkably, AR-mediated transcription with *R*-3 is enhanced in the T877A mutant form, where both the Br-M895 and the water bridged *R*-3–L873 interactions are present.

It is possible that to observe the full destabilization of the HF/AR WT system, a longer MD timeframe should be considered. The presence of co-repressors might also shift the unstable HR/AR WT system to the antagonist conformation [33].

By looking at these data, it can be also predicted that the point mutations T877A and W741L do not have an effect on the binding of *R*-bicalutamide and HF, respectively. These two ligands, in fact, remain antagonists towards these respective mutations explaining the useful ortogonality of these two drugs used in prostate cancer patients.

4. Conclusions

We performed 2.15 ns of MD simulations on several non-steroidal-bound AR complexes (WT and mutant forms) to study the molecular basis for ligand agonicity and antagonicity in the AR, and the change in biological activity upon subtle modifications in the ligands and/or the receptor (mutations). This constitutes the first attempt to incorporate protein dynamics in this analysis, which complements a previous study performed from static crystal structures [18,19].

In the antagonist *R*-bicalutamide/AR WT complex, we found strong evidence that M895 (located in H12) destabilization by both W741 and the sulfonyl linkage of *R*-bicalutamide might be responsible for reported antagonism. We also confirmed that changes in the sulfonyl linker by a smaller ether one (*S*-1, model **2**), or a mutation in the receptor (AR W741L complexed with *R*-bicalutamide, model **6**), allow M895 to stably pack onto *S*-1 and L741, respectively, thus stabilizing the receptor in the agonist conformation. Moreover, the M895T mutation has been reported as *R*-bicalutamide resistant [19]. No internal hydrogen bond was observed between the amide hydrogen and the ether linkage in *S*-1 in models **2** and **3**, and the sulfonyl oxygen of *R*-bicalutamide (model **6**), in disagreement with what had been originally supposed [19]. In the *S*-1/AR W741L complex (model **3**), we found that the presence of a water molecule linking the side chain of N705 (H3) and the hydroxyl group of *S*-1 helps to stabilize the complex.

The HF/AR WT complex (model **7**) displayed a weaker interaction pattern between HF and M895 (H12) and higher instability when compared with the AR T877A mutant (model **8**). In the latter, the water molecule bridging the ligand and the backbone of L873 (H11) adds stability to the system, while at the same time, the interaction with M895 becomes stronger.

We observed that antagonists HF and *R*-bicalutamide introduce a certain degree of dynamic instability in the AR WT agonist-bound conformation, mostly stemming from weaker or lack of interactions between the ligand and residues in H5, H11 or H12, or destabilization of residues therein. Whether this translates into H12 relocation, or it can be explained in passive antagonism terms, it would premature to assess. Our results explain the role of specific point mutations as T877A and W741L in antagonist resistance, and provide a valuable framework for structure-based design of ligands which antagonize both mutant and the WT AR for the prevention and the cure of still untreatable stages of prostate cancer.

Acknowledgments

William Bisson acknowledges support from the Swiss National Science Foundation. The authors thank Sharangdhar Phatak (UTHSC-H) for help with the manuscript.

Appendix A. Supplementary data

Supplementary data associated with this article can be found, in the online version, at doi:10.1016/j.jmgm.2008.08.001.

References

[1] S.P. Balk, Urology 60 (2002) 132.
[2] H. Miyamoto, E.M. Messing, C. Chang, Prostate 61 (2004) 332.
[3] H. Gronemeyer, J.A. Gustafsson, V. Laudet, Nat. Rev. Drug Discov. 3 (2004) 950.
[4] T. Hara, J. Miyazaki, H. Araki, M. Yamaoka, N. Kanzaki, M. Kusaka, M. Miyamoto, Cancer Res. 63 (2003) 149.
[5] M.E. Taplin, S.P. Balk, J. Cell Biochem. 91 (2004) 483.
[6] A.O. Brinkmann, J. Trapman, Nat. Med. 6 (2000) 628.
[7] S. McDonald, L. Brive, D.B. Agus, H.I. Scher, K.R. Ely, Cancer Res. 60 (2000) 2317.
[8] X.Y. Zhao, P.J. Malloy, A.V. Krishnan, S. Swami, N.M. Navone, D.M. Peehl, D. Feldman, Nat. Med. 6 (2000) 703.
[9] J.P. Renaud, D. Moras, Cell Mol. Life Sci. 57 (2000) 1748.
[10] A.K. Shiau, D. Barstad, J.T. Radek, M.J. Meyers, K.W. Nettles, B.S. Katzenellenbogen, J.A. Katzenellenbogen, D.A. Agard, G.L. Greene, Nat. Struct. Biol. 9 (2002) 359.
[11] A. Souque, J. Fagart, B. Couette, E. Davioud, F. Sobrio, A. Marquet, M.E. Rafestin-Oblin, Endocrinology 136 (1995) 5651.
[12] L. Nagy, J.W. Schwabe, Trends Biochem. Sci. 29 (2004) 317.

[13] P. Carlsson, K.F. Koehler, L. Nilsson, Mol. Endocrinol. 19 (2005) 1960.
[14] L.D. Alvarez, M.A. Marti, A.S. Veleiro, D.M. Presman, D.A. Estrin, A. Pecci, G. Burton, J. Med. Chem. 51 (2008) 1352.
[15] L. Celik, J.D. Lund, B. Schiott, Biochemistry 46 (2007) 1743.
[16] J. Zeng, W. Li, Y. Zhao, G. Liu, Y. Tang, H. Jiang, J. Phys. Chem. B 112 (2008) 2719.
[17] S. Burendahl, E. Treuter, L. Nilsson, Biochemistry 47 (2008) 5205.
[18] C.E. Bohl, W. Gao, D.D. Miller, C.E. Bell, J.T. Dalton, Proc. Natl. Acad. Sci. U.S.A. 102 (2005) 6201.
[19] C.E. Bohl, D.D. Miller, J. Chen, C.E. Bell, J.T. Dalton, J. Biol. Chem. 280 (2005) 37747.
[20] C.E. Bohl, Z. Wu, D.D. Miller, C.E. Bell, J.T. Dalton, J. Biol. Chem. 282 (2007) 13648.
[21] W.H. Bisson, C.N. Cavasotto, R.A. Abagyan, The Role of Point Mutations Causing Antiandrogen Withdrawal Syndrome Studied by Molecular Simulations and Computational Prediction Approaches, Basel, Switzerland, 2005, MipTec, May 9–12, 2005.
[22] C.N. Cavasotto, R.A. Abagyan, J. Mol. Biol. 337 (2004) 209.
[23] C.N. Cavasotto, G. Liu, S.Y. James, P.D. Hobbs, V.J. Peterson, A.A. Bhattacharya, S.K. Kolluri, X.K. Zhang, M. Leid, R. Abagyan, R.C. Liddington, M.I. Dawson, J. Med. Chem. 47 (2004) 4360.
[24] C.N. Cavasotto, A.J.W. Orry, R. Abagyan, Proteins: Struct. Funct. Bioinf. 51 (2003) 423.
[25] D.A. Case, T.A. Darden, T.E. Cheatham III, C.L. Simmerling, J. Wang, R.E. Duke, R. Luo, K.M. Merz, B. Wang, D.A. Pearlman, M. Crowley, S. Brozell, V. Tsui, H. Gohlke, J. Mongan, V. Hornak, G. Cui, P. Beroza, C. Schafmeister, J.W. Caldwell, W.S. Ross, P.A. Kollman, Amber 8, University of California, San Francisco, 2004.
[26] A. Di Nola, D. Roccatano, H.J.C. Berendsen, Proteins: Struct. Funct. Genet. 19 (1994) 174.
[27] J. Wang, P. Morin, W. Wang, P.A. Kollman, J. Am. Chem. Soc. 123 (2001) 5221.
[28] W. Wang, P.A. Kollman, Proc. Natl. Acad. Sci. U.S.A. 98 (2001) 14937.
[29] M.M. van Lipzig, A.M. ter Laak, A. Jongejan, N.P. Vermeulen, M. Wamelink, D. Geerke, J.H. Meerman, J. Med. Chem. 47 (2004) 1018.
[30] J.H. Wu, B. Gottlieb, G. Batist, T. Sulea, E.O. Purisima, L.K. Beitel, M. Trifiro, Hum. Mutat. 22 (2003) 465.
[31] C.A. Marhefka, B.M. Moore 2nd, T.C. Bishop, L. Kirkovsky, A. Mukherjee, J.T. Dalton, D.D. Miller, J. Med. Chem. 44 (2001) 1729.
[32] P.M. Matias, P. Donner, R. Coelho, M. Thomaz, C. Peixoto, S. Macedo, N. Otto, S. Joschko, P. Scholz, A. Wegg, S. Basler, M. Schafer, U. Egner, M.A. Carrondo, J. Biol. Chem. 275 (2000) 26164.
[33] M.S. Ozers, B.D. Marks, K. Gowda, K.R. Kupcho, K.M. Ervin, T. De Rosier, N. Qadir, H.C. Eliason, S.M. Riddle, M.S. Shekhani, Biochemistry 46 (2007) 683.